Modeling Study on Absorption of CO$_2$ by Aqueous Solutions of *N*-Methyldiethanolamine in Rotating Packed Bed

Zhi Qian, Lianbin Xu, Huibo Cao, and Kai Guo*

Research Center of the Ministry of Education for High Gravity Engineering and Technology, Beijing University of Chemical Technology, Beijing 100029, PR China

The work presents a theoretical investigation of the absorption of CO$_2$ by aqueous solutions of *N*-methyldiethanolamine (MDEA) in a rotating packed bed (RPB). The diffusion-reaction process for CO$_2$-MDEA mass transfer in RPB is modeled according to Higbie's penetration theory with the assumption that all reactions are reversible. A three-dimensional distribution of carbon dioxide concentration varying with the time and penetration depth in liquid film and an average mass transfer rate at interface are obtained. The intensification within the RPB is mainly achieved by the sharper concentration profile of the dissolvable gas in liquid film; the short lifetime of liquid film resulting from frequent renewal of the film on packing surface significantly increases the mass transfer coefficient. Experiments were carried out at various rotating speeds, liquid flow rates, and temperatures in RPB. The validity of this model is demonstrated by the fact that most of the predicted y_{out} (mole fraction of CO$_2$ in outlet gas) agree well with the experimental data with a deviation within 4%. Besides, this study makes a quantitative comparison between dynamic- and static-state mass transfer coefficients for this reactive absorption and a discussion on their applicability.

1. Introduction

The removal of carbon dioxide (CO$_2$) and hydrogen sulphide (H$_2$S) from natural and refinery gases is usually accomplished by using aqueous alkanolamine solutions. In industrial gas processing, there is an increasing interest in gas absorption process for the selective removal of H$_2$S from gas mixtures. Among the alkanolamines, aqueous solutions of *N*-methyldiethanolamine (MDEA), due to its higher H$_2$S selectivity,[1] are frequently used to selectively absorb H$_2$S from gas streams containing both CO$_2$ and H$_2$S. Since the rate of reaction of MDEA with H$_2$S is instantaneous while the rate of reaction of the alkanolamine with CO$_2$ is relatively slower, the selectivity of H$_2$S is controlled by the rate of reaction of the amine with CO$_2$.[2] Obviously, this process requires a minimum contact time to avoid unwanted, time-dependent reactions. Therefore, a rotating packed bed (RPB) is seemingly ideal for the selective H$_2$S removal from gases that need a "short" contactor.[3]

As a novel and highly efficient contactor, RPB utilizes centrifugal acceleration to intensify the mass transfer[4,5] and has been applied to absorption, distillation, polymer devolatilization, and reactive crystallization, etc.[6−9] According to previous studies, the RPB has higher gas−liquid mass transfer efficiency which is evidenced by the fact that the volumetric mass transfer coefficients within a PRB are an order of magnitude higher than those in a conventional packed bed. Recently, RPB has been used to absorb CO$_2$ with aqueous solutions of alkanolamine and effects of various operation parameters on the absorption performances were investigated.[10,11]

The reaction of CO$_2$ with the MDEA is the control step of the selectivity of H$_2$S in a RPB.[3] Modeling and experimental studies on absorption of CO$_2$ by aqueous solutions of MDEA in a RPB should be made. Several investigations have already been made on the performance of countercurrent gas−liquid mass transfer in RPB.[12−18] A viewpoint that the intensification is achieved by a larger gas−liquid effective interfacial area being produced under centrifugal field is widely accepted. The liquid flow in a RPB has been supposed to be laminar film flow on the packing surface and the thickness of the film has been figured out.[13,14,19,20] The thinner films resulting from a large centrifugal acceleration can expand the gas−liquid contact surface area and increase the mass transfer rate. However, visual observations reported by Ramshaw and Burns[21] indicated a maldistribution of liquid within the packing. In fact, it is extremely hard to quantify the effective gas−liquid mass transfer area because of the complexity of liquid flow in RPB. Hence, a model reflecting the reactive absorption process in RPB more directly and realistically should be developed.
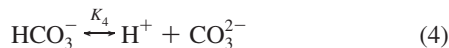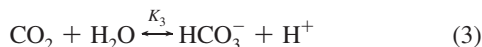
In this work, the absorption of CO$_2$ by aqueous solutions of MDEA in a RPB is studied theoretically and experimentally. By weighing the pros and cons of the effects on increasing the gas−liquid interfacial areas, the authors of this study hold that it is relatively reliable to regard the surface areas of packing as the effective ones for mass transfer. The intensification within the RPB is mainly achieved by the sharper concentration profile of the dissolvable gas in liquid film, because the short lifetime of liquid film resulting from its frequent renewal on packing surface significantly increases the mass transfer coefficient. Then a model based on Higbie's penetration theory with the assumption that all reactions are reversible is established to describe the mechanism of gas−liquid mass transfer accompanied with reactions in a RPB. Experiments of CO$_2$ absorption by MDEA solution in the RPB at various operation conditions were carried out as well. The experimental data well confirm to the theoretical model developed in this paper.

2. Reactions of CO$_2$ in Aqueous MDEA Solutions

When CO$_2$ is absorbed into an aqueous solution of MDEA, several equilibrium reactions occur in the solution, which are as follows

$$CO_2 + R_3N + H_2O \xrightleftharpoons[\quad\quad]{k_{2,MDEA}, K_1} R_3NH^+ + HCO_3^- \quad (1)$$
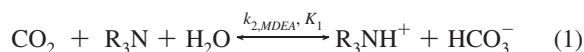
* To whom correspondence should be addressed. Tel. and fax: +86-10-64448808. E-mail: guok@mail.buct.edu.cn.

$$R_3N + H^+ \overset{K_2}{\longleftrightarrow} R_3NH^+ \tag{2}$$

$$CO_2 + H_2O \overset{K_3}{\longleftrightarrow} HCO_3^- + H^+ \tag{3}$$

$$HCO_3^- \overset{K_4}{\longleftrightarrow} H^+ + CO_3^{2-} \tag{4}$$

$$CO_2 + OH^- \overset{k_{OH^-}, K_5}{\longleftrightarrow} HCO_3^- \tag{5}$$

$$H_2O \overset{K_6}{\longleftrightarrow} H^+ + OH^- \tag{6}$$

MDEA is easily protonized and the corresponding reaction in the solution is expressed by eq 2.

Among reactions 1−6, reactions 1, 3, and 5 have influence on the absorption of carbon dioxide. However, it is well-known that the rate of reaction 3 is very slow and may usually be neglected.[22] In this paper, it is assumed that there is a fast reversible reaction of CO_2 and OH^- in parallel, i.e., reaction 5 with another rapid pseudo-first-order reversible reaction between CO_2 and MDEA, i.e., reaction 1. They are following the base catalysis mechanism[23] and zwitterion mechanism,[24] respectively.

For the absorption of CO_2 in MDEA aqueous solutions, the overall reaction rate of CO_2 can be expressed in terms of reversible reactions giving the generally accepted expression

$$r_{ov} = k_{2,MDEA} c_{R_3N} c_{CO_2} - \frac{k_{2,MDEA}}{K_1} c_{R_3NH^+} c_{HCO_3^-} + k_{OH^-} c_{OH^-} c_{CO_2} - \frac{k_{OH^-}}{K_5} c_{HCO_3^-} \tag{7}$$

When chemical equilibrium is reached for reactions 1 and 5, equilibrium equations can be expressed as

$$k_{2,MDEA} c_{R_3N} c_{CO_2,eq} = \frac{k_{2,MDEA}}{K_1} c_{R_3NH^+} c_{HCO_3^-} \tag{8}$$

$$k_{OH^-} c_{OH^-} c_{CO_2,eq} = \frac{k_{OH^-}}{K_5} c_{HCO_3^-} \tag{9}$$

where $c_{CO_2,eq}$ is the equilibrium concentration of CO_2. The reaction rate for a reverse reaction can be evaluated by considering conditions at equilibrium and it is generally true even when the system is not at equilibrium.[25] The net forward rate of reaction can be deduced from eq 7.

$$r_{ov} = k_{2,MDEA} c_{R_3N} (c_{CO_2} - c_{CO_2,eq}) + k_{OH^-} c_{OH^-} (c_{CO_2} - c_{CO_2,eq}) \tag{10}$$

$c_{CO_2,eq}$ can be calculated from reactions 2 and 3 and written as

$$c_{CO_2,eq} = \frac{1}{K_2 K_3} \frac{c_{R_3NH^+} c_{HCO_3^-}}{c_{R_3N}} \tag{11}$$

The overall balance for MDEA is

$$c_{R_3N,total} = c_{R_3NH^+} + c_{R_3N} \tag{12}$$

$c_{R_3N,total}$ is total liquid bulk concentration of MDEA. Therefore, eq 12 can be rewritten as

$$c_{CO_2,eq} = \frac{1}{K_2 K_3} \frac{(c_{R_3N,total} - c_{R_3N}) c_{HCO_3^-}}{c_{R_3N}} \tag{13}$$

Because of a small loading of CO_2 in amine, the OH^- concentration can be estimated from the relations given by Astarita.[26]

$$c_{OH^-} = \sqrt{\frac{K_w}{K_p} c_{R_3N}} \tag{14}$$

where K_w and K_p are water dissociation constant and MDEA protonation constant, respectively.

From eq 10, the overall reaction rate constant k_{ov} has the following expression

$$k_{ov} = k_{2,MDEA} c_{R_3N} + k_{OH^-} c_{OH^-} \tag{15}$$

3. Gas−Liquid Mass Transfer Accompanied by Reversible Reactions

3.1. Assumption. 1. According to the study of Basic and Dudukovic[19] and Guo Kai,[27] the liquid flow in RPB has been assumed to be laminar film flow on the packing surfaces. Majorities of the liquid in the RPB exist in the form of liquid film and on which the mass transfer takes place.

2. The surface areas of packing are regarded as the gas−liquid effective interfacial ones.

3. The rotor in RPB consists of 31 layers of packing. Liquid film is renewed every time it passes through one layer of packing. The mean lifetime of liquid film in each layer is the same and determined by both liquid residence time and total number of packing layers.

3.2. Model Development. 3.2.1. Modeling of the Gas−liquid Mass Transfer Coefficient in the High Gravitational Field. It is known that the OH^- concentration is constant in a liquid film from eq 14 and k_{ov} can be assumed as a constant in each liquid film. Since the conversion of R_3N into R_3NH^+ is very low in a thin film, c_{R_3N} and $c_{HCO_3^-}$ are also assumed as a constant. Consequently, the equilibrium concentration of CO_2 could be treated as a constant according to eq 13. The physicochemical properties and kinetic data have been well-known and determined as discussed by Rinker et al.[1] and Ko.[22] For brevity, they are not repeated here. The partial differential equation describing the diffusion of CO_2 into liquid film accompanied by the pseudo-first-order reversible chemical reaction is

$$\begin{cases} \dfrac{\partial c_{CO_2}}{\partial t} = D_{CO_2} \dfrac{\partial^2 c_{CO_2}}{\partial x^2} - k_{ov}(c_{CO_2} - c_{CO_2,eq}), 0 < x < \infty, t > 0 \\ \text{B.C.} c_{CO_2}(0, t) = c_{CO_2,0}, c_{CO_2}(\infty, t) \le c_{CO_2,eq} \end{cases} \tag{16}$$

$c_{CO_2,0}$, determined by $(p^i_{CO_2})/(H_{CO_2})$, is the concentration of CO_2 at the gas−liquid interface and $c_{co_2,eq}$ is the equilibrium concentration of CO_2 for the reaction.

Letting $c_A = c_{CO_2} - c_{CO_2,eq}$ and with Laplace transform, we obtain an ordinary differential equation.

$$\begin{cases} D_{CO_2} \dfrac{d^2 \tilde{c}_A}{d\tilde{x}^2} - (s + k_{ov}) \tilde{c}_A = 0 \\ \text{B.C.} \tilde{c}_A(0, s) = \dfrac{c_{CO_2,0} - c_{CO_2,eq}}{s}, \tilde{c}_A(\infty, s) \le 0 \end{cases} \tag{17}$$

The solution to eq 17 is

$$\tilde{c}_A(x, s) = \frac{c_{CO_2,0} - c_{CO_2,eq}}{s} \exp\left(-x\sqrt{\frac{s + k_{ov}}{D_{CO_2}}}\right) \quad (18)$$

Using Laplace inverse transform we obtain an analytical expression for the concentration distribution of CO_2 as a function of time and penetration depth in liquid film.

$$c_{CO_2} = \frac{c_{CO_2,0} - c_{CO_2,eq}}{2} \exp\left(-x\sqrt{\frac{k_{ov}}{D_{CO_2}}}\right) \mathrm{erfc}\left(\frac{x}{2\sqrt{D_{CO_2}t}} - \sqrt{k_{ov}t}\right) +$$
$$\frac{c_{CO_2,0} - c_{CO_2,eq}}{2} \exp\left(x\sqrt{\frac{k_{ov}}{D_{CO_2}}}\right) \mathrm{erfc}\left(\frac{x}{2\sqrt{D_{CO_2}t}} + \sqrt{k_{ov}t}\right) + c_{CO_2,eq} \quad (19)$$

where erfc(x) is excess error function. The mass transfer rate at the gas−liquid interface is calculated from the first Fick law.

$$R_{CO_2} = -D\frac{\partial c_{CO_2}}{\partial x}\bigg|_{x=0} = (c_{CO_2,0} - c_{CO_2,eq}) \times$$
$$\left[\sqrt{\frac{D_{CO_2}}{\pi t}}\exp(-k_{ov}t) + \sqrt{k_{ov}D_{CO_2}}\mathrm{erf}(\sqrt{k_{ov}t})\right] \quad (20)$$

where erf(x) is error function. The liquid film is renewed when it passes through the packing layer and the renewal frequency is determined by

$$S = u \cdot \frac{N_S}{R_1 - R_2} \quad (21)$$

where N_S is the number of layers of the wire-meshed packing, 31 in this study, while R_2, R_1 are the outer and inner radius of the packing, respectively. The u is the average radial flow rate of the liquid film.[28]

$$u = 0.02107L^{0.2279}(\omega R)^{0.5448} \quad (22)$$

where L is liquid flux. Then the mean lifetime of the liquid film can be gotten by

$$\bar{t} = \frac{1}{S} \quad (23)$$

Due to the assumption that the lifetime of liquid film on each packing layer is the same, the Higbie age distribution function of mass transfer in the liquid film can be defined as

$$\psi(t) = \frac{1}{\bar{t}}, 0 < t < \bar{t} \quad (24)$$

From eqs 20 and 24 the expression of the time-averaged mass transfer rate of CO_2 per unit interfacial area can be written as

$$\bar{N}_{CO_2} = \int_0^{\bar{t}} R_{CO_2} \cdot \psi(t)dt = \frac{\sqrt{k_{ov}D_{CO_2}}}{\bar{t}} \times$$
$$\left[\bar{t}\mathrm{erf}(\sqrt{k_{ov}\bar{t}}) + \sqrt{\frac{\bar{t}}{\pi k_{ov}}}\exp(-k_{ov}\bar{t}) + \frac{1}{2k_{ov}}\mathrm{erf}(\sqrt{k_{ov}\bar{t}})\right] \times$$
$$(c_{CO_2,0} - c_{CO_2,eq}) \quad (25)$$

The liquid-side mass transfer coefficient (k_L) can be calculated from the following equation

$$\bar{N}_{CO_2} = k_L(c_{CO_2,0} - c_{CO_2,eq}) \quad (26)$$

Therefore, the analytic expression of k_L is written as

$$k_L = \frac{\sqrt{k_{ov}D_{CO_2}}}{\bar{t}}\left[\bar{t}\mathrm{erf}(\sqrt{k_{ov}\bar{t}}) + \sqrt{\frac{\bar{t}}{\pi k_{ov}}}\exp(-k_{ov}\bar{t}) + \frac{1}{2k_{ov}}\mathrm{erf}(\sqrt{k_{ov}\bar{t}})\right] \quad (27)$$

3.2.2. Quantitative Comparison between Dynamic- and Static-State Mass Transfer Processes. Equation 27 in the previous section is the mass transfer coefficient expression for the dynamic-state mass transfer, a static-state one can be deduced from dual film theory by modeling absorption of CO_2 into MDEA solution on a wetted-wall column, i.e., gravity flow

$$\begin{cases} D_{co_2}\dfrac{d^2c_{CO_2}}{dx^2} = k_{ov}(c_{CO_2} - c_{CO_2,eq}) \\ \mathrm{B.C.}c_{CO_2}(x = 0) = c_{CO_2,0}, c_{CO_2}(x = \delta) = c_{CO_2,eq} \end{cases} \quad (28)$$

$C_{CO_2,0}$, determined by $(p^i_{CO_2})/(H_{CO_2})$, is the concentration of CO_2 at the gas−liquid interface and $C_{co_2,eq}$ is the equilibrium concentration of CO_2 for the reaction.

From first Fick's Law, the mass transfer rate at the gas−liquid interface is

$$N_{CO_2} = D_{CO_2}\frac{dC_{CO_2}}{dx}\bigg|_{x=0} = k_L^0(c_{CO_2} - c_{CO_2,eq})\frac{Ha}{th(Ha)} \quad (29)$$

where

$$Ha = \frac{1}{k_L^0}\sqrt{k_{ov}D_{CO_2}} \quad (30)$$

k_L^0 is the liquid-side mass transfer coefficient of the physical absorption of CO_2 by water.

For $Ha > 3$,[22] the value of tanh(Ha) becomes approximately unity. Then eq 29 can be simplified as

$$N_{CO_2} = \sqrt{k_{ov}D_{CO_2}}(c_{CO_2} - c_{CO_2,eq}) \quad (31)$$

Then the liquid-side mass transfer coefficient for the static-state process can be expressed as

$$k_L = \sqrt{k_{ov}D_{CO_2}} \quad (32)$$

The quantitative comparison between dynamic- and static-state mass transfer coefficients for absorption CO_2 into MDEA solution is written below

$$\frac{k_{L,dynamic}}{k_{L,static}} = \frac{\left[\bar{t}\mathrm{erf}(\sqrt{k_{ov}\bar{t}}) + \sqrt{\dfrac{\bar{t}}{\pi k_{ov}}}\exp(-k_{ov}\bar{t}) + \dfrac{1}{2k_{ov}}\mathrm{erf}(\sqrt{k_{ov}\bar{t}})\right]}{\bar{t}} \quad (33)$$

3.2.3. Gas−Liquid Mass Transfer in RPB. Pacheco and Rochelle[29] considered that gas-film resistance was never significant for CO_2 absorption into MDEA solution. Furthermore, Trent and Tirtowidjojo[30] and Guo et al.[31] held promise for significant intensification of gas-side mass transfer in RPB. Considering the previous study, it was supposed that there was little resistance in gas-side for CO_2 absorption into MDEA solution in the RPB. For the analysis above and no accurate values of k_G available now, this absorption process in the RPB

was based on the assumption that the gas-phase resistance was negligible, i.e., $P_{CO_2}^i = P_{CO_2}$.

In this one-dimensional mass transfer model, the concentration of every component varies only in the radial direction of the packing because liquid and gas have little circumferential motion.[21] Liquid motion in RPB hardly has back mixing, so the liquid radial flow is close to plug flow.[18] On the basis of the above analysis, a differential mass balance can be employed in gas phase for CO_2

$$k_y\alpha\left(y - \frac{H}{P}\frac{1}{K_2 K_3}\frac{(c_{R_3N,total} - c_{R_3N})c_{HCO_3^-}}{c_{R_3N}}\right)2\pi hRdR =$$
$$G_{N_2}d\left(\frac{y}{1-y}\right) \quad (34)$$

According to the reaction stoichiometry, differential mole balances for HCO_3^- and R_3N are

$$k_L\alpha\frac{P}{H}\left(y - \frac{H}{P}\frac{1}{K_2 K_3}\frac{(c_{R_3N,total} - c_{R_3N})c_{HCO_3^-}}{c_{R_3N}}\right)2\pi hRdR =$$
$$Qd(c_{HCO_3^-}) \quad (35)$$

$$-k_L\alpha\frac{P}{H}\left(y - \frac{H}{P}\frac{1}{K_2 K_3}\frac{(c_{R_3N,total} - c_{R_3N})c_{HCO_3^-}}{c_{R_3N}}\right)2\pi hRdR =$$
$$Qd(c_{R_3N}) \quad (36)$$

y is the mole fraction at the gas−liquid interface, $k_y = 0.082 \cdot T \cdot k_L(P)/(H)$, α is the specific area of the packing, P is the total pressure of the system, H is Herry constant for absorption of CO_2 into MDEA, G_{N_2} is the flow rate of N_2. Q is the liquid flow rate. It is assumed as a constant because the increase in liquid mass is tiny as the liquid moves outward.

4. Method of Solution

Equations 34, 35, and 36 are integrated from the outer to the inner edge of packing in RPB. This differential equation set belongs to a boundary-value problem. However, it can be converted into an initial-value problem by getting initial values from solving algebraic equations.

To approximate the solution of differential equations, the initial values of y, $c_{HCO_3^-}$ and c_{R_3N} over the radial length of packing [0, 0.052] need to be determined. The mole fraction of CO_2 inlet gas, $y(0) = 0.1$ is known. The $c_{HCO_3^-}(0)$ and $c_{R_3N}(0)$ can be estimated from the total concentration of MDEA, the CO_2 loading of the MDEA solution, and the assumption that all reactions are at equilibrium at liquid outlet. We have the following equations for the liquid bulk concentrations $c_{R_3NH^+}^0$, $c_{R_3N}^0$, $c_{CO_2}^0$, $c_{HCO_3^-}^0$, $c_{CO_3^{2-}}^0$, $c_{OH^-}^0$, and $c_{H^+}^0$.

Overall balance for MDEA

$$c_{R_3N,total} = c_{R_3NH^+}^0 + c_{R_3N}^0 \quad (37)$$

With the CO_2 loading of aqueous MDEA solution, α_{CO_2}, in kmol CO_2/kmol MDEA, the overall CO_2 balance is

$$c_{R_3N,total}\alpha_{CO_2} = c_{CO_2}^0 + c_{HCO_3^-}^0 + c_{CO_3^{2-}}^0 \quad (38)$$

The charge balance is

$$c_{R_3NH^+}^0 + c_{H^+}^0 = c_{OH^-}^0 + c_{HCO_3^-}^0 + 2c_{CO_3^{2-}}^0 \quad (39)$$

In the reaction scheme 2−6, four equilibrium constants, K_2, K_3, K_4, and K_6, are independent. The other can be obtained by an appropriate combination of these independent equilibrium constants. The equilibrium constants of reactions 2−4 and 6 are as follows

$$K_2 = \frac{c_{R_3NH^+}^0}{c_{R_3N}^0 c_{H^+}^0} \quad (40)$$

$$K_3 = \frac{c_{HCO_3^-}^0 c_{H^+}^0}{c_{CO_2}^0} \quad (41)$$

$$K_4 = \frac{c_{CO_3^{2-}}^0 c_{H^+}^0}{c_{HCO_3^-}^0} \quad (42)$$

$$K_6 = c_{H^+}^0 c_{OH^-}^0 \quad (43)$$

The seven algebraic eqs 37−43 are solved for the concentrations in the bulk liquid at liquid outlet, $c_{R_3NH^+}^0$, $c_{R_3N}^0$, $c_{CO_2}^0$, $c_{HCO_3^-}^0$, $c_{CO_3^{2-}}^0$, $c_{OH^-}^0$ and $c_{H^+}^0$. The Newton method is usually used, but it is complicated with the error propagation. In this study, the dichotomy is applied to solve the equations. We introduce an implicit function with the unknown $c_{H^+}^0$, which ranges from 0 to 1 mol/L determined by pH indicator. The equilibrium constants needed to solve the mathematical model have been well-known and determined as discussed by Zhang Xu.[32]

For convenience, the concentrations of chemical species are renamed as follows

$$b_1 = c_{R_3N,total}, \, b_2 = c_{R_3N,total}\alpha, \, x_1 = c_{R_3NH^+}^0, \, x_2 = c_{R_3N}^0,$$
$$x_3 = c_{CO_2}^0, \, x_4 = c_{HCO_3^-}^0, \, x_5 = c_{CO_3^{2-}}^0, \, x_6 = c_{OH^-}^0, \, x_7 = c_{H^+}^0$$

An implicit function for x_7 is obtained by solving eqs 37 − 43,

$$\frac{K_2 \cdot b_1 \cdot x_7}{1 + K_2 \cdot x_7} + x_7 - \frac{b_2}{\frac{x_7}{K_3} + 1 + \frac{K_4}{x_7}} -$$
$$2 \cdot \frac{K_4}{x_7} \cdot \frac{b_2}{\frac{x_7}{K_3} + 1 + \frac{K_4}{x_7}} - \frac{K_6}{x_7} = 0 \quad (44)$$

Equation 44 was solved by the dichotomy programmed with FORTRAN for x_7, and the error was within the last step length. Other data can be obtained by inversion. Here, $c_{HCO_3^-}(0) = x_4$ and $c_{R_3N}(0) = x_2$. The Runge−Kutta−Fehlberg method (denoted RKF45) is employed to solve the model equations with the three initial values. Figure 1 shows the solutions of differential equations, which are $y(R')$, $y_{eq}(R')$, $c_{HCO_3^-}(R')$, and $c_{R_3N}(R')$ over $R' \in [0, 0.052]$ respectively, describing the absorption of CO_2 by 10% MDEA at 293 K and 1100 r/min in RPB.

5. Experimental Section

Figure 2 illustrates the experimental apparatus for the CO_2 absorption into MDEA. The RPB employed in this study had an inner diameter of 42 mm, an outer diameter of 146 mm, and a height of 20 mm. The stainless wire mesh was used as the packing with a specific area of 500 m^2/m^3 and a voidage of 97%. The total volume of the packing was 307 cm^3. The packing consisted of 31 layers. The nitrogen stream containing CO_2
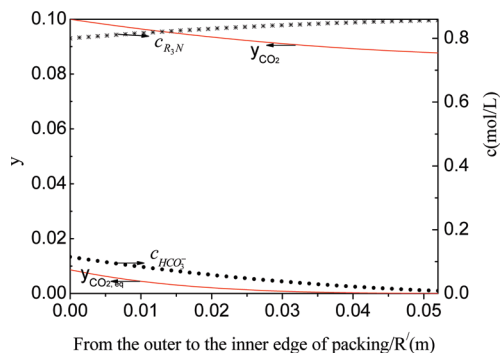
Figure 1. Solutions of differential equations for the absorption of CO_2 by 10% MDEA at 293 K and 1100 r/min in RPB.
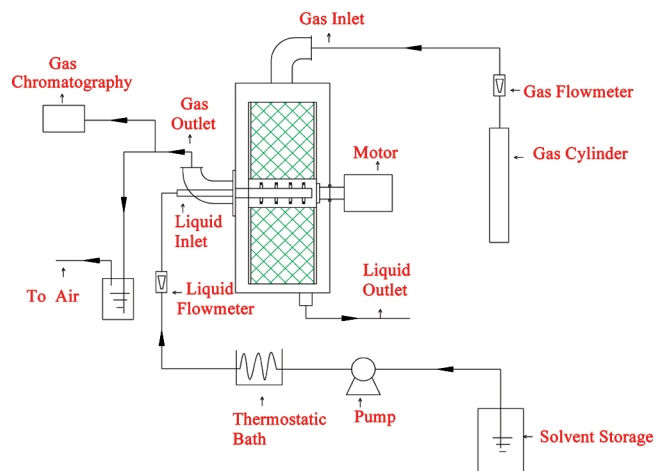

Figure 2. Experimental flowchart for the CO_2 absorption into MDEA.

flowed inward from the outer edge of the RPB by pressure and the aqueous absorbent was sprayed onto the inner edge of the RPB via a distributor. The aqueous absorbent moved outward and left from the outer edge of the RPB by centrifugal force. CO_2 in the gas stream was dissolved and reacted with MDEA while gas and liquid contacted countercurrently in the RPB. The inlet gas had a flow rate of 1100 L/h. The rotating speeds varied from 600 to 1300 r/min. For all runs, a steady-state operation was reached within 2 min. The CO_2 concentrations in the inlet and outlet gas streams were measured by gas chromatography (SP-2100, BAIF Chromatograph Instrument Center). CO_2 mole fraction ranged from 0 to 10%. The CO_2 loading of the amine solution was determined by standard titration methods. The operation temperatures were maintained at 293, 303, and 313 K respectively via thermostatic bath, and the pressure was ambient pressure. The aqueous solutions of MDEA were prepared by distilled−deionized water and the concentration of MDEA in the solutions was determined by titration with HCl. All the experiments were conducted in the concentration range of 10−30 mass% MDEA.

6. Results and Discussion

6.1. Effects of Rotating Speed, Liquid Flow Rate, and Temperature. Figures 3 and 4 show the dependence of y_{out} and the predicted k_L on the rotating speed, liquid flow rate, and temperature under the operation conditions of 10% MDEA solution, inlet CO_2 mole fraction of 10%. It is seen that y_{out} declines and k_L increases with an increase in the rotating speed in the range from 600 to 1300 r/min and the liquid flow rate from 6 to 10 L/h, which means that the lifetime of liquid film shortens with an increase in rotating speed or liquid flow rate.
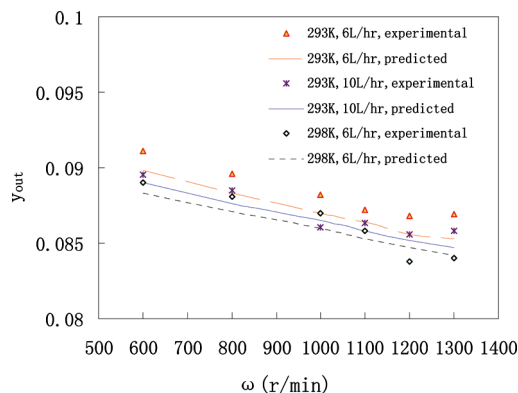

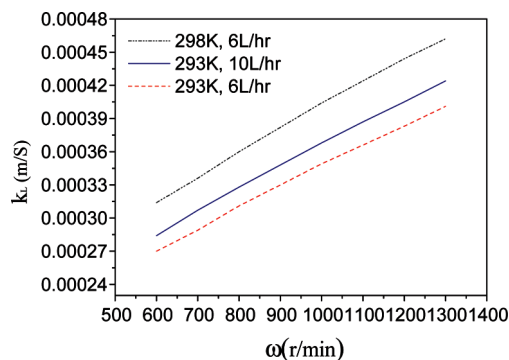**Figure 3.** Effects of rotating speed, liquid flow rate, and temperature on y_{out}.

Figure 4. Effects of rotating speed, liquid flow rate, and temperature on k_L.

It is also seen from Figures 3 and 4 that the temperature has a significant effect on y_{out} and k_L and both of them change a lot as the temperature rises from 293 to 298 K, indicating that the process of absorption of CO_2 into MDEA solution is sensitive to temperature. This is attributed to a higher temperature resulting in a higher k_{ov} according to the Arrhenius expression of reaction rate constant. Hence, it is beneficial to a higher mass transfer coefficient of liquid phase and removal efficiency of dissolvable gas by increasing temperature to some extent besides decreasing lifetime of liquid film for a reactive absorption. In addition, Figure 3 also shows the predicted trend line and there is good agreement between the experimental and theoretical values.

6.2. Lifetime of Liquid Film and Three-Dimensional Distribution of CO_2 Concentration in Liquid Film. According to eq 19, a picture of distribution of CO_2 concentration in liquid film can be drawn. For the absorption of CO_2 by 10% MDEA under the operation conditions of rotating speed of 1100 r/min, liquid flow rate of 6 L/h, and temperature of 293 K, the concentration distribution of CO_2 in the liquid film which varies with the time, t, and the penetration depth, x, is shown as Figure 5. The liquid film does not disappear until its lifetime exceeds 0.015 s and another concentration profile is built, which causes a large mass transfer coefficient. Figure 5 only exhibits the case of the distribution of CO_2 concentration in liquid films as the films flowing through three layers of packing. Obviously, the less mean lifetime of liquid film, the sharper the concentration profile and the bigger the mass transfer coefficient. In addition, the mole fraction of CO_2 in gas corresponding to its concentration on gas−liquid interface decreases gradually with the increase of time as the boundary in Figure 5 shows.
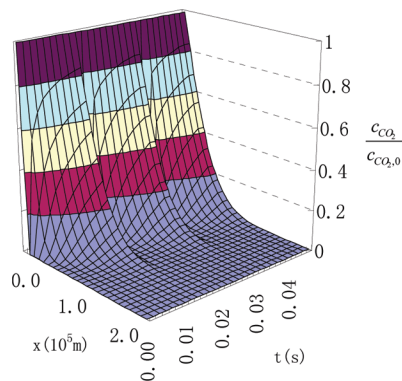
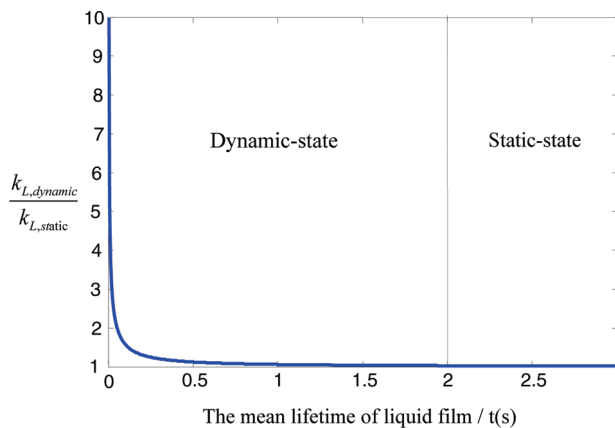**Figure 5.** Concentration distribution of CO_2 in the liquid film.

Figure 6. Comparison between dynamic- (high gravity flow) and static-state (gravity flow) mass transfer coefficients for absorption of CO_2 into 10% MDEA.

6.3. Comparison between Dynamic- and Static-State Mass Transfer Coefficients. Figure 6 illustrates that the mass transfer coefficient rises as the mean lifetime of liquid film decreases, i.e., the rotating speed of the RPB increases, at temperature of 293 K and fluid flow rate of 6 L/h. When the mean lifetime is longer than 2 s, the mass transfer coefficient gradually becomes irrelevant to the mean lifetime of the liquid film and dynamic-state mass transfer is converted into static-state one. The longer the mean lifetime, the closer to the static-state for the mass transfer process. For the absorption of CO_2 by 10% MDEA at temperature of 293 K and fluid flow rate of 6 L/h, given $\bar{t}$ = 2 s, the ratio $(k_{L,dynamic})/(k_{L,static})$ is 1.02. When the mean lifetime of liquid film is shorter than 2 s, a strong intensification effect will be imposed on the mass transfer. As the plot shows, the intensification increases sharply with a decline of the time and makes the dynamic-state mass transfer a great difference from the static-state one. Once the mean lifetime of the liquid film shrinks approximately to 0, the intensification can expand to infinity which means that the liquid-phase resistance is zero. For a static appliance, such as wetted-wall column, if liquid flows quite fast on the column, the residence time will be very short. In this case, an obvious error will emerge if the dual film model is applied to simulate the mass transfer process. Here, the residence time, as one of the important factors impacting the process, should be taken into consideration. Also, the quantitative comparison indicates that the short lifetime of liquid film can significantly intensify the gas−liquid reactive absorption.

6.4. Model Validation. In the case of knowing the physicochemical properties, kinetic data[1,22] and lifetime of liquid film, the CO_2 composition in outlet gas could be obtained
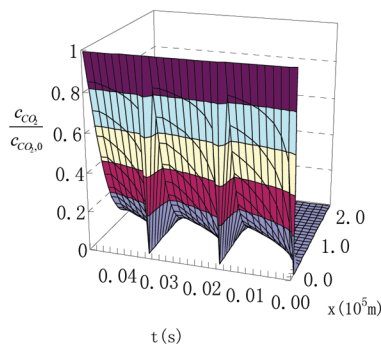

Figure 7. Diagonal graph of experimental and predicted y_{out}.

according to differential eqs 34−36. Figure 7 is the diagonal plot of the predicted and experimental values of CO_2 composition in outlet gas under the operation conditions of gas flow rate of 1100 L/h, liquid flow rate of 6 L/h, rotating speeds in the range from 600 to 1300 r/min, operation temperatures maintained at 293, 303, and 313 K respectively, and MDEA in the concentration range of 10−30%. It can be found that this model offers relatively precise predictions on CO_2 mole fraction in outlet gas, with a deviation of 4% compared to the experimental values.

7. Conclusion

The intensification within RPB is mainly achieved by the sharper concentration profile of the dissolvable gas in liquid film because of the very short lifetime of liquid film on the packing surface. The shorter the mean lifetime of liquid film, the bigger the mass transfer coefficient. Based on Higbie's penetration theory, the analytical expression of the concentration distribution of CO_2 as a function of time and penetration depth in liquid film, and that of the gas−liquid mass transfer coefficient in RPB are obtained. A mathematical model is developed in this work to quantitatively describe the gas−liquid mass transfer process with reversible reactions in a RPB. The mole fraction of CO_2 in outlet gas predicted by the model is in a good agreement with the experimental data at various liquid flow rates, rotating speeds, and temperatures. The effects of various operation parameters on the mass transfer coefficient in RPB are predicted reasonably by this model. In addition, a quantitative comparison between dynamic- and static-state mass transfer coefficients also indicates that the short lifetime of liquid film because of renewal can significantly intensify the gas−liquid reactive absorption and increase the mass transfer coefficient.

Appendix

Nomenclature

D = diffusivity, m^2/s

G = volumetric flow rate of gas, m^3/s

G_{N_2} = flow rate of N$_2$, m^3/s

g = gravitational constant, m/s^2

H = solubility of gas in solution, kPa m^3/kmol

Ha = Hatta number as defined by eq 14

h = height of packing, m

K = equilibrium constant

$k_{2,MDEA}$ = second-order reaction rate constant, m^3/kmol s

k_L = liquid-phase mass transfer coefficient, m/s

k_{OH^-} = reaction rate constant for CO$_2$ hydration, m^3/kmol s

k_{ow} = overall pseudo-first-order reaction rate constant, 1/s

L = liquid flux, m/s

N_{CO_2} = time-averaged mass transfer rate of CO$_2$ per unit interfacial area, kmol/m^2 s

P_{CO_2} = a partial pressure of CO$_2$ in the gas phase, kPa

$P_{CO_2}^i$ = a partial pressure of CO$_2$ in the gas phase at the gas−liquid interface, kPa

Q = volumetric flow rate of the liquid, m^3/s

R = geometrical mean radius

R' = radial length of packing from 0 to 0.52, m

R_{out} = outer radius of rotator in RPB, m

R_{in} = inner radius of rotator in RPB, m

r = reaction rate, kmol/m^3 s

s = complex variable

T = temperature, K

$\bar{t}$ = mean lifetime of the liquid film, s

y = mole fraction of CO$_2$ in gas

y_{in} = mole fraction of CO$_2$ inlet gas

y_{out} = mole fraction of CO$_2$ outlet gas

Greek letters

α = specific area, m^2/m^3

ω = rotating speed, r/min

Abbreviations

MDEA = methyldiethanolamine

R$_3$N = MDEA

R$_3$H$^+$ = protonized MDEA

Acknowledgment

Literature Cited

(1) Rinker, E. B.; Ashour, S. S.; Sandall, O. C. Kinetics and modelling of carbon dioxide absorption into aqueous solutions of N-methyldiethanolamine. *Chem. Eng. Sci.* **1995**, *50* (5), 755–768.

(2) Versteeg, G. F.; van Swaaij, W. P. M. b. On the kinetics between CO$_2$ and alkanolamines both in aqueous and non-aqueous solutions-II. Tertiary amines. *Chem. Eng. Sci.* **1988**, *43* (3), 587–591.

(3) Bucklin B. W.; Won, K. W. Higee contactors for selective H$_2$S removal and superdehydration. Laurance Reid Gas Conditioning Conference, University of Oklahoma, March 2−4, 1987.

(4) Ramshaw, C. Mass transfer process. European Patent No. 0002568, 1979.

(5) Ramshaw, C. The opportunities for exploiting centrifugal fields. *Heat Recovery Syst. CHP* **1993**, *13* (6), 493–513.

(6) Stephen, C. S.; Kermit, E. W.; Howard, S. M.; Fowller, R., Selective acid gas removal using the Higee absorber. AIChE Spring meeting, Orlando, FL, March18−22, 1990.

(7) Martin, C. L.; Martelli, M. Preliminary distillation mass transfer and pressure drop results using a pilot scale high gravity contacting unit. AIChE Spring Meeting, New Orleans, LA, March 29−April 2,1992.

(8) Gardner, N. C. Polymer devolazation by rotating packed bed. The first international workshop high gravity engineering and technology, Beijing, China, June 1996.

(9) Chen, J.; Wang, Y.; Zheng, C.; Jia, Z. Synthesis of nano particles of CaCO3 in a novel reactor. The second international conference on process intensification in practice, Antwerp, Belgium, October 21−23, 1997.

(10) Lin, C. C.; Liu, W. T.; Tan, C. S. Removal of carbon dioxide by absorption in a rotating packed bed. *Ind. Eng. Chem. Res.* **2003**, *42*, 2381–2386.

(11) Tan, C. S.; Chen, J. E. Absorption of carbon dioxide with piperazine and its mixtures in a rotating packed bed. *Sep. Purif. Technol.* **2006**, *49*, 174–180.

(12) Tung, H. H.; Mah, R. S. H. Modelling liquid mass transfer in HIGEE separation process. *Chem. Eng. Commun.* **1985**, *39*, 147–153.

(13) Munjal, S.; Dudukovic, M. P.; Ramachandran, P. A. Mass transfer in rotating packed beds−I. Development of gas-liquid and liquid-solid mass transfer correlations. *Chem. Eng. Sci.* **1989**, *44*, 2245–2256.

(14) Munjal, S.; Dudukovic, M. P.; Ramachandran, P. A. Mass transfer in rotating packed beds−II. Experimental results and comparison with theory and gravity flow. *Chem. Eng. Sci.* **1989**, *44*, 2257–2268.

(15) Kumar, M. P.; Rao, D. P. Studies on a high-gravity gas-liquid contactor. *Ind. Eng. Chem. Res.* **1990**, *29*, 917–920.

(16) Ding, X. L. A model for the mass transfer coefficient in rotating packed bed. *Chem. Eng. Commun.* **2000**, *178*, 249–256.

(17) Chen, Y. S.; Lin, C. C.; Liu, H. S. Mass Transfer in a Rotating Packed Bed with Viscous Newtonian and Non-Newtonian Fluids. *Ind. Eng. Chem. Res.* **2005**, *44*, 1043–1051.

(18) Yi, F.; Zou, H. K.; Chu, G. W.; Shao, L.; Chen, J. F. Modeling and experimental studies on absorption of CO$_2$ by Benfield solution in rotating packed bed. *Chem. Eng. J.* **2009**, *145*, 377–384.

(19) Basic, A.; Dudukovic, M. P. Liquid holdup in rotating packed bed: examination of the film flow assumption. *AIChE J.* **1995**, *41*, 301–316.

(20) Guo, K.; Guo, F.; Feng, Y.; Chen, J.; Zheng, C.; Gardner, N. C. Synchronous visual and RTD study on liquid flow in rotating packed-bed contactor. *Chem. Eng. Sci.* **2000**, *55*, 1699–1706.

(21) Burns, J. R.; Ramshaw, C. Process intensification: visual study of liquid maldistribution in rotating packed beds. *Chem. Eng. Sci.* **1996**, *51* (8), 1347–1352.

(22) Ko, J. J.; Li, M. H. Kinetics of absorption of carbon dioxide into solutions of N-methyldiethanolamine+water. *Chem. Eng. Sci.* **2000**, *55*, 4139–4147.

(23) Donaldson, T. L.; Nguyen, Y. N. Carbon dioxide reaction kinetics and transport in aqueous amine membranes. *Ind. Eng. Chem. Fundam.* **1980**, *19*, 260–266.

(24) Yu, W. C.; Astarita, G.; Savage, D. W. Kinetics of carbon dioxide absorption in solutions of methyldiethanolamine. *Chem. Eng. Sci.* **1985**, *40*, 1585–1590.

(25) Danckwerts, P. V. *Gas-Liquid Reactions*; McGraw-Hill: New York, 1970.

(26) Astarita, G.; Savage, D. W.; Bisio, A. *Gas treating with chemical solvents*; Wiley: New York, 1983.

(27) Guo, K. A study on liquid flowing inside the Higee rotor. Ph.D Dissertation, Beijing University of Chemical Technology, 1996.

(28) Chen, J. F. *High Gravity Technology and Application*; Chemical Industry Press of China, 2002.

(29) Pacheco, M.; Rochelle, G. T. Rate-based modeling of reactive absorption of CO$_2$ and H$_2$S into aqueous Methyldiethanolamine. *Ind. Eng. Chem. Res.* **1998**, *37*, 4107–4117.

(30) Trent, D.; Tirtowidjojo, D. Commercial operation of a rotating packed bed (RPB) and other application of RPB technology. *Better Processes for Better Products, 4th International Conference on Process Intensification for the Chemical Industry*, Brugge, Belgium, 2001; pp 11−19.

(31) Guo, F.; Zheng, C.; Guo, K.; Feng, Y.; Gardner, N. C. Hydrodynamics and mass transfer in cross flow rotating packed bed. *Chem. Eng. Sci.* **1997**, *52*, 3853–3859.

(32) Zhang, X.; Zhang, C. F.; Liu, Y. Kinetics of absorption of CO$_2$ into aqueous solution of MDEA blended with DEA. *Ind. Eng. Chem. Res.* **2002**, *41*, 1135–1141.